Hindawi
Journal of Nanomaterials
Volume 2022, Article ID 4136072, 11 pages
https://doi.org/10.1155/2022/4136072

Research Article

Preparation and Properties of Functional Materials Based on Digital Light Processing 3D Printing

Weiping Deng,[1] **Deqiao Xie**,[2] **Fuxi Liu**,[1] **Lida Shen**,[1,3] **Zongjun Tian**,[1,3] **and Yang Yang**[4]

[1]*College of Mechanical and Electrical Engineering, Nanjing University of Aeronautics and Astronautics, Nanjing, 210016 Jiangsu, China*
[2]*College of Energy and Power Engineering, Nanjing University of Aeronautics and Astronautics, Nanjing 210016, Jiangsu, China*
[3]*National Key Laboratory of Science and Technology on Helicopter Transmission, Nanjing University of Aeronautics and Astronautics, Nanjing, 210016 Jiangsu, China*
[4]*General Manager of Huaxin New Material (Zhuzhou) Co., Ltd, Zhuzhou, 412000 Hunan, China*

Correspondence should be addressed to Weiping Deng; wpdeng@nuaa.edu.cn

Received 24 March 2022; Revised 22 June 2022; Accepted 7 July 2022; Published 16 August 2022

Academic Editor: Awais Ahmed

3D printing, known as the "new industrial revolution," has set off an upsurge in the scientific and technological field in recent years, and 3D printing of digital light processing technology has even improved the performance and efficiency of 3D printing. This technology uses the projection principle to form; no matter the size of the workpiece, the forming speed is not affected. It uses very cheap lamp radiation, the system has no injection-molded components, there is no nozzle clogging problem of traditional molding systems, and maintenance costs are greatly reduced. In this paper, based on digital light processing 3D printing technology, light-curing reactive functional materials commonly used in digital light processing 3D printing are prepared. In the past, most of these materials were imported. In this paper, by adjusting the DLP technology, a water-soluble photocurable reflection material is constructed, a method for shaping the reaction material. It conducts experiments on the preparation and performance research of water-soluble photocurable reaction materials through formulation and process optimization. It prepared a water-soluble photocurable reactive functional material and compared it with traditional imported materials. Due to the characteristics of UV curing and good mechanical properties and water solubility, it provides a new idea for the preparation of 3D printing-related functional materials.

1. Introduction

Digital light processing (DLP) refers to digitally processing an image signal and then projecting it to the desired point. In 3D printing, because of its high-precision casting technology, it can achieve excellent performance in material, detail, and surface material casting.

Nowadays, there are many types of 3D printing materials, the common ones are ABS, PLA, and Nylon. There are many more, such as resins under DLP/SLA molding technology and metals (such as aluminum, iron, steel, silver, gold, and titanium) for industrial-grade models, ceramics, etc. There are also various materials with special properties, such as magnetic materials, conductive materials, wood-like materials, elastic materials, and hard materials like concrete, special inks for bio-3D printing. These materials are suitable for different application fields and show their own characteristics, and 3D printing of functional materials is also included in this category.

Functional materials refer to materials with excellent electrical, magnetic, optical, thermal, and other functions and special physical, chemical, and biological effects, which can complete the mutual transformation of functions, and are mainly used to construct various functions. Because 3D printing has the advantages of short manufacturing cycle, high molding precision, and customization, the technology is widely used in many aspects, and printing materials are the key. Among them, the vacancy of photocurable reactive functional materials as supporting materials has affected the development of digital light

processing 3D printing technology in China. In this paper, with digital light processing technology as the core, a water-soluble photocurable 3D printing reactive material was prepared and studied. This is of great significance for the development of digital light processing technology 3D printing and related functional materials. The innovation is that it can make up for the current situation of relying on imports of this material and play a certain reference role in promoting the development of related materials in China.

2. Related Work

Due to the increasing popularity of 3D printing, 3D printing-related technologies are becoming an emerging core competitiveness. Huang and Lin combined the "Conceive, Design, Implement, Operate" (CDIO) framework with 3D printing tangible to propose a novel technical thinking [1]. Xu et al. developed a framework to study the innovation capabilities of multilayer innovation ecosystems involving science, technology, and business subecosystems. They selected China's 3D printing ecosystem as a case study, in addition to analyzing the interplay between the science, technology, and business layers [2]. Vanderburgh et al. highlighted recent advances in 3D printing of tissue-engineered structures. They defined it as the layer-by-layer fabrication of a part guided by digital information in a 3D computer-aided design file. In this structure, they recapitulated the physical and cellular properties of the tissue microenvironment and it was used to study disease progression mechanisms and screen drugs [3]. Xu et al. proposed a combination of 3D scanning and cement mortar-based 3D printing for developing a new process for replicating decorative parts of historic buildings. The process was traditionally labor-intensive and expensive to build, but they developed and presented a layered algorithm for model slicing and an improved scanline algorithm for nozzle paths [4]. Ho et al. prepared stereolithography (STL) format computer models and contrast-enhanced CT of 3D printed models for 3D printing in the medical field. Their proposed 3D-printed model, generated from a strong and flexible plastic material, successfully replicated the anatomical details of the aortic structure and pathology [5]. The printability of the materials used in extrusion-based 3D printing was one of the most important properties, especially when manufacturing objects of architectural complexity. However, this parameter is affected by several factors (temperature, composition, and additives), which makes comprehensive evaluation and classification challenging. Kim et al. evaluated the printability of food inks for 3D food printing applications by systematically adjusting dimensional stability testing, handling performance evaluation, and shear rheology testing using edible hydrocolloids as reference materials. Thus, a high-quality solution is proposed [6]. To date, most printable thermoset materials suffer from complex processes, poor thermodynamic properties, and slow printing speeds. Wang et al. developed a photosensitive composite ink for fast photocuring printing, which has a good auxiliary role for 3D printing under digital light processing [7]. However, the photosensitive composite ink they developed is lacking in the accuracy of 3D printing and is prone to errors in more complex model processing tasks, so it still needs to be improved before it is widely used.

3. Technical Setup and Material Preparation Method of 3D Printing Based on Digital Light Processing

DLP 3D printing based on digital light processing mainly uses DMD chips developed by TI. It uses a high-pixel digital light processor (DMD) optomechanical to project model slices to solidify liquid photopolymer layer by layer [8]. In a DLP projection system, the core element is its DMD chip. The DMD chip can deflect the microscope to different angles to complete the light modulation [9]. The size of the DMD micromirror is generally 7.6 μm, the minimum is 5.4 μm, and the maximum is 13.6 μm. There are two types of arrangement: square arrangement and rhombus arrangement. In order to facilitate the deflection of the mirror, there is a certain gap between the arrays, so the actual size of the chip and the projection size are not only determined by the size of the mirror [10]. Figure 1 shows the layout of the lower exposure 3D printing system and DMD chip lens.

3.1. DLP Technology Adjustment. When DLP technology is applied to 3D printing, the reflectivity and diffraction performance of the DMD chip microprocessor can be affected due to the higher photoresponse of the photoinitiator in the photosensitive material to higher energy light. The energy rate of the system also has an effect [11]. Excessive use of light energy can cause excessive system losses, fail to reach projection targets, or even damage equipment. Therefore, the reflectivity of the DMD chip in different light zones, as well as in the DMD window, will be the main estimate.

According to the DMD chip guidance given by TI, DMD chips suitable for visible light, ultraviolet light, and near-infrared wavelengths also have different energy utilization rates for different light wavelengths under different human radiation angles, as shown in Figure 2.

The DMD window is optimized by coating for the wavelength of 420~700 nm in the visible light band to improve the transmission efficiency. The ultraviolet band is optimized for the light wavelength of 355~400 nm, and the optimized effect is shown in Figure 3.

In 3D printing applications, the typical wavelengths used by DLP technology are 355 nm and 405 nm, mainly determined by the light source [12]. The optimization effect of visible light band and ultraviolet light band in Figure 3 shows that the DMD chip for ultraviolet band should be used as the core of the system. It ensures that the system has a high light energy consumption rate. If the visible light region DMD chip is used, the system loss will increase. If the wavelength of the light source is 355 nm, the utilization rate is only 70%, and the waste of system energy is huge [13]. After completing the above settings, it can print the material. The specific process is shown in Figure 4.

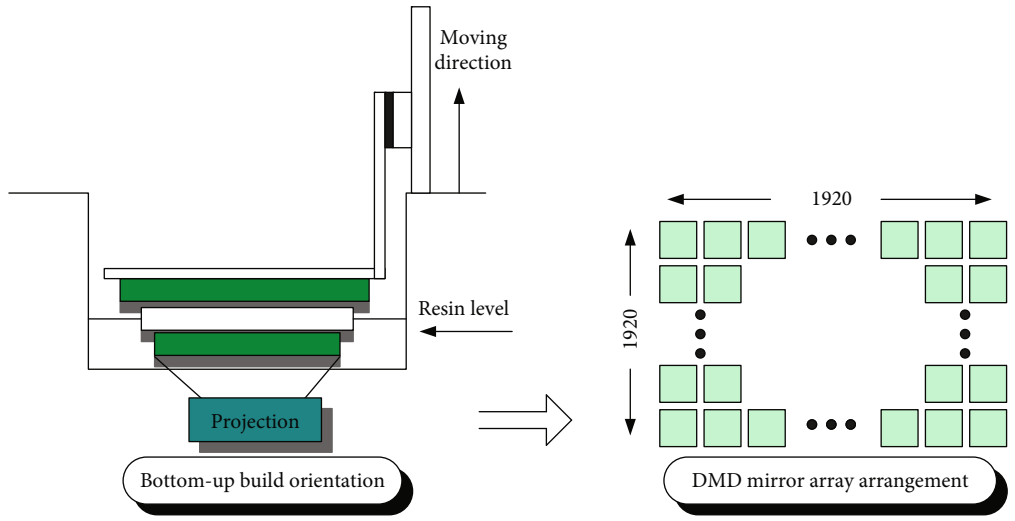

Figure 1: Layout of the lower exposure 3D printing system and DMD chip lens.

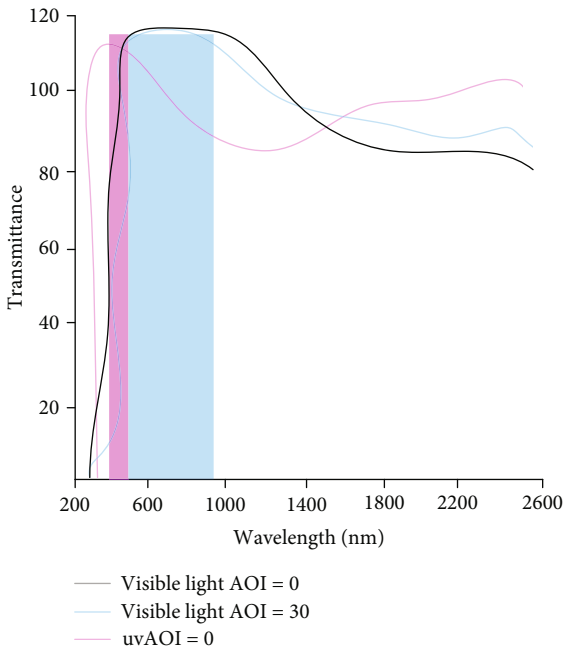

Figure 2: Energy utilization curve of DMD chip at different wavelengths.

After understanding the working principle and operation process of DLP technology, the next article will introduce the curing and molding mechanism of the functional materials to be prepared. It studies the effect of process conditions on the properties of the material before and after curing to determine the optimal formulation of the material. This provides a certain theoretical basis and practical methods for the localization of digital light processing 3D printing materials.

3.2. Construction Principle of Water-Soluble Photoreactive Materials. Light-curing 3D printing materials are composed of a solid material and a support material. The material responsible for building the solid part of the part is called the solid material. It directly affects the molding accuracy and surface quality of solid parts and is a key functional material for photocuring 3D printing [14]. The composition of the material includes prepolymer, monomer, and photoinitiator, as shown in the following formula. The polymerization cross-linking reaction allows the liquid resin to form a cured product in a very short time:

$$\begin{aligned} X - Y &\xrightarrow{\text{hv}} \left(\frac{X}{Y}\right), \\ \left(\frac{X}{Y}\right) \cdot &\longrightarrow X \cdot + Y. \end{aligned} \tag{1}$$

It abstracts hydrogen atoms from hydrogen atom donors such as prepolymers and active monomers, such as photoinitiator ITX, to make them active free radicals. After the previous step is completed, as shown in the following formula, the polymerization and cross-linking reaction is further initiated.

$$\begin{aligned} X &\xrightarrow{\text{hv}} X, \\ X \cdot &\xrightarrow{RH} XH + R. \end{aligned} \tag{2}$$

The photocurable reactive materials mainly include three stages of chain initiation, chain growth, and chain termination [15].

(1) Chain initiation

The photoinitiator (I) absorbs light energy under the irradiation of a UV lamp. It transitions from the ground state to the excited state, forming active radicals (R). The active free radical then undergoes an addition reaction with the monomer (M) to form a monomer free radical, as shown

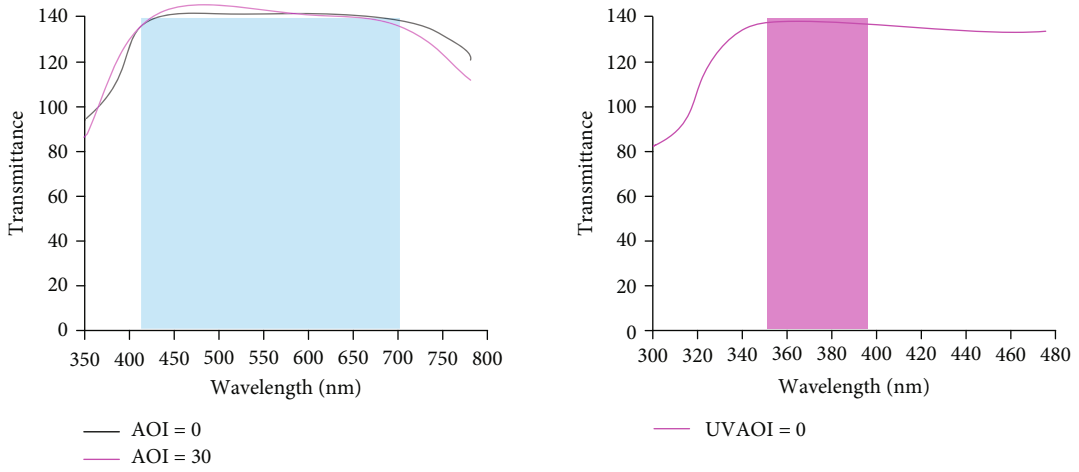

Figure 3: Optimization effect diagram of visible light band and ultraviolet light band.

in the formula:

$$I \xrightarrow{hv} R,$$
$$R \cdot + M \xrightarrow{hv} (R - M). \tag{3}$$

(2) Chain growth

The above process is repeated continuously, so that active radicals and monomers are rapidly added to form macromolecules. Light-curing printing materials change from liquid to solid:

$$(R\text{-}M)_n \cdot + M \xrightarrow{hv} (R - M - M)_n \cdot \tag{4}$$

(3) Chain termination

Common chain terminations include disproportionation termination and coupling termination. With the continuous progress of the chain growth reaction, the content of free radicals in the chain increases continuously, and the photocuring reaction ends [16].

3.3. Curing and Characterization of Reactive Materials

(1) Viscosity

The viscosity of the reactive material is measured according to the specified standard. It puts an appropriate amount of liquid reaction material into the barrel of the digital viscometer and then puts the barrel into a constant temperature water tank. It uses a No. 21 rotor to measure the viscosity of the reaction material at different temperatures [17].

Viscosity is an important process parameter characterizing the jetting properties of photocurable 3D printing support materials, which determines whether the reactive material can be smoothly and steadily ejected from the nozzle [18]. It is subjected to shearing force. It simplifies the injection process, and the viscosity of the reaction material is shown in the formula:

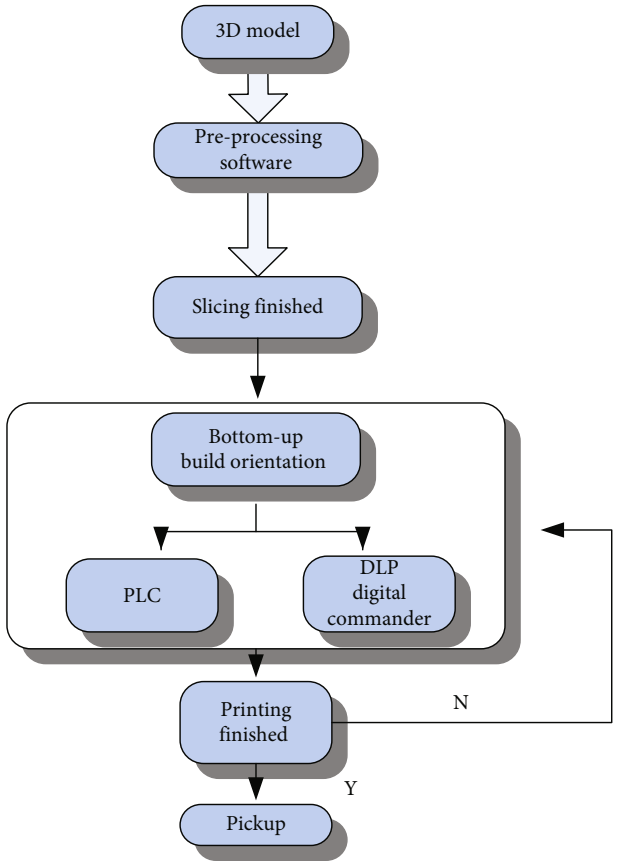

Figure 4: DLP printing process.

$$\tau = F|A,$$
$$D = \left(\frac{dx}{dz}\right)|dt, \tag{5}$$
$$\eta = \tau|D.$$

τ is the shear stress, F is the shear force, A is the area where the shear force acts, and D is the shear rate. dx/dz is the shear deformation, dt is the shear force action time, and η is the viscosity of the reaction material.

(2) Surface tension

It measures the surface tension of the reactive material. It puts an appropriate amount of liquid temperature-sensitive reactive material sample into the barrel of the automatic surface tensiometer and then puts the barrel into a constant temperature water tank. It chooses the platinum plate method to test the surface tension of the reaction material at different temperatures. The specific process is as follows:

$$P = \mathrm{mg} + L\gamma(\cos\theta) - sh\rho g. \tag{6}$$

(3) Volatilization rate

It adds the reaction material to the beaker. The mass of the beaker is M_0, and the total mass after adding the reaction material is M_1. After being placed at different temperatures for different times, it measured a total mass of M_2. The volatilization rate α of the reaction material is calculated as follows:

$$\alpha = \frac{M_1 - M_2}{M_1 - M_0}. \tag{7}$$

(4) Curing shrinkage

Under the condition of 25°C, it uses the ZMD-2 electronic densitometer to measure the density of the reaction material before curing and the density of the cured product, and the curing shrinkage can be calculated by the formula:

$$\Delta = \frac{\rho_1 - \rho_0}{\rho_0}. \tag{8}$$

(5) Solubility

It cuts the cured product of the reaction material to obtain a sample with a size of $10 \times 10 \times 4\,\mathrm{mm}^3$. The mass of the sample is called M_0, and the sample is soaked in distilled water of different temperatures for a certain period of time. It takes a filter paper with a quality of M_1 for filtration and puts the filter paper and the sample into a vacuum drying oven for drying, and the quality after drying is M_2. Then, the reaction material solubility S is calculated by the following formula:

$$S = \frac{M_0 - (M_2 - M_1)}{M_0}. \tag{9}$$

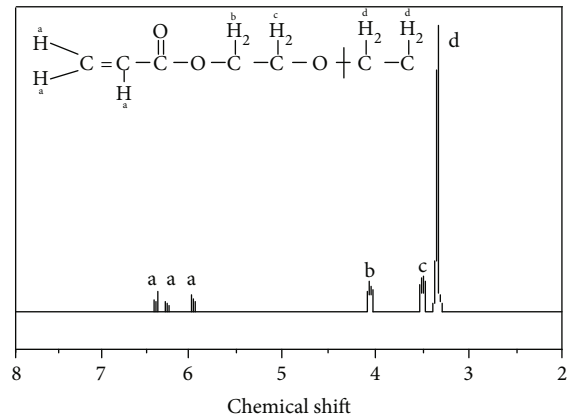

Figure 5: 1H NMR spectrum of single-end hydroxyl PEGmA.

The photocuring reaction process of the photocurable monomer is as follows:

$$\begin{aligned} R &\xrightarrow{\text{violetray}} R, \\ R\cdot + \text{mPEG400DA} &\longrightarrow R - \text{PEG400DA}_m, \\ R\cdot + R - \text{PEG400DA}_m\cdot &\longrightarrow R - \text{PEG400DA}_m - R, \\ R - \text{PEG400DA}_m\cdot + R - \text{PEG400DA}_m\cdot &\longrightarrow R - \text{PEG400DA}_m - R. \end{aligned} \tag{10}$$

R is a photoinitiator, R is a free radical, and PEG400DA is polyethylene glycol 400 diacrylate.

Surface tension is also an important process parameter for light-cured 3D printing reaction materials, which determines whether the reaction materials can be smoothly and stably ejected from the nozzle [19]. During jet printing, the reactive material droplets have a tendency to automatically shrink into spherical shapes. The air resistance and the change of the mass of the reaction material droplets are ignored, and the force of the reaction material is simplified. The surface tension of the reactive material is shown in the formula:

$$\alpha = \frac{\omega}{\gamma}. \tag{11}$$

In the formula, α is the surface area of the new surface, ω is the work done when the new surface is generated, and γ is the surface tension coefficient.

3.3.1. Experiments on the Preparation and Performance of Water-Soluble Photocurable Reactive Materials. Before the experiment, the water-soluble photocurable monomer must first be provided for the preparation of the water-soluble photocurable 3D printing reaction material. Single-ended hydroxyl PEGmA, also known as polyethylene glycol acrylate monoester, has good UV curing properties. Because of its special molecular structure, PEGmA and its cured products have good water solubility and can be easily removed by water gun [20]. In addition, PEGmA has the advantages of nontoxicity and low volatilization rate. Therefore,

Table 1: Basic formula of water-soluble photocurable 3D reactive materials.

Materials	PEGmA	Polyethylene glycol	369	ITX	Other agents
Proportion of the 1st blend/wt%	75	12	2	2	9
Proportion of the 2nd blend/wt%	65	12	2	2	8
Proportion of the 3rd blend/wt%	43	6	2	1	7
Proportion of the 4th blend/wt%	22	6	1	1	6
Proportion of the 5th blend/wt%	15	3	1	1	4

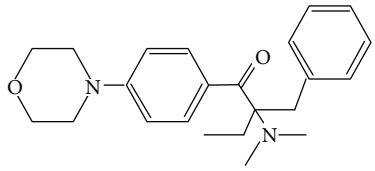

Figure 6: Schematic diagram of the structure of photoinitiator 369.

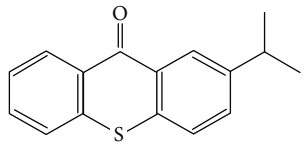

Figure 7: Schematic diagram of the structure of the photoinitiator ITX.

PEGmA provides a new idea for the preparation of water-soluble photocurable reactive materials. However, it is currently difficult to purchase pure PEGmA in the market, and the domestic synthesis process and purification method of PEGmA are not mature, and there is no commercial PEGmA, so it is necessary to make PEGmA.

3.4. Synthesis and Purification of Single-Ended Hydroxyl PEGmA. It firstly adds a certain amount of reactant polyethylene glycol into a 250 ml container equipped with a thermometer, a constant pressure dropping funnel, a water separator, and a condenser. In the flask, it heated the mixture to 60°C with magnetic stirring. After the p-toluenesulfonic acid and hydroquinone were completely dissolved, the temperature was raised to 120°C. It continues to magnetically stir for 10 to 15 minutes, and after no bubbles are produced, it filters. The filtered product was added to a rotary evaporator, distilled under reduced pressure, and toluene was removed to obtain a crude product of PEGmA.

It uses a pipette to, respectively, measure a certain amount of reaction solution and distilled water (mass ratio 1 : 10) into a conical flask, add indicator phenolphthalein, and mix evenly. It is titrated to a reddish color with standard NaOH solution, shaken, and the end point of the titration is that the red color does not fade within 30 seconds. It records the amount of NaOH solution consumed and calculates the acidity and esterification of the sample.

The formula for calculating acidity is as follows:

$$\mathrm{AV} = \frac{\mathrm{CVMr}}{m_s}. \tag{12}$$

In the formula, AV is the acidity value of the sample; C is the mass concentration of the standard NaOH solution; V is the volume of the NaOH solution consumed when the titration reaches the end point; Mr is the relative molecular mass of NaOH; m_s is the mass of the sample taken.

The calculation of the degree of esterification of the esterification reaction is as follows:

$$\mathrm{DE} = \frac{A_i - A_t}{A_i}. \tag{13}$$

Among them, DE is the esterification degree of the sample; A_i is the initial acidity value of the sample; A_t is the acidity value of the sample measured at a certain time.

Figure 5 is the 1H NMR spectrum of single-ended hydroxyl PEGmA. It can be seen from Figure 5 that, compared with pure polyethylene glycol, characteristic peaks appear at the chemical shifts of 5.8-6.5 in the hydrogen spectrum of single-end hydroxyl PEGmA, corresponding to the 3 Hs of the terminal alkenyl group. The characteristic peaks at chemical shifts 4.2-4.4 correspond to the 2 Hs on the carbon atom of the ester group and the 2 Hs on the methylene group connected to the terminal hydroxyl group. It has characteristic peaks at chemical shifts of 3.6-3.8. The characteristic peaks at chemical shifts of 3.5 to 3.6 correspond to 82 Hs in the oxyethane structure of the monoester, which indicates that the oxyethane structure (ether chain structure) of polyethylene glycol is not destroyed. In conclusion, the esterification reaction of polyethylene glycol and acrylic acid occurred to generate single-end hydroxyl PEGmA. The peak shape in the figure is sharp, and there are few impurity peaks, which proves that the purity of the monoester is high.

3.5. Preparation of Reactive Photocurable 3D Printing Materials. Single-end hydroxyl PEGmA has excellent UV curability and can be cured quickly under the action of photoinitiator. And its cured product has good water solubility and mechanical properties, which can support the molding of solid materials [21]. After it has been formed, the PEGmA cured product can be removed by flushing with a water gun. Therefore, PEGmA meets the performance of water-soluble functional materials, which provides a new idea for the preparation of water-soluble photocurable 3D printing materials. In this section, on the basis of the synthesized water-soluble PEGmA as the photocurable monomer, a new type of water-soluble functional material, reactive photocurable 3D printing functional material, was prepared. It analyzes the influence of monomers, types, and contents

Table 2: The volatilization rate of reaction materials containing 75 wt% PEGmA in different environments.

Storing time	8	16	24	32	40	48	56	64	72
Wet environment	0.18	0.24	0.29	0.33	0.48	0.40	0.59	0.60	0.69
Dry environment	0.15	0.23	0.26	0.29	0.38	0.39	0.49	0.56	0.68
Hot environment	0.28	0.33	0.39	0.47	0.51	0.55	0.62	0.68	0.72
Cold environment	0.01	0.12	0.2	0.35	0.38	0.52	0.64	0.65	0.68

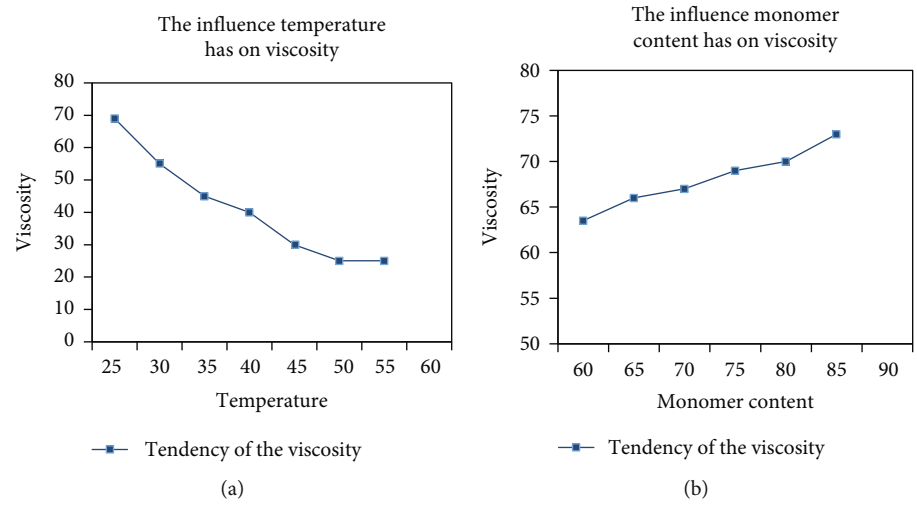

Figure 8: Effect of temperature and monomer content on viscosity of reaction material.

of photoinitiators on the properties of the material, studies the preparation process of the material, and analyzes its curing and forming mechanism. It finalizes the optimal formulation of water-soluble photocurable 3D reactive materials. The basic formula is shown in Table 1.

It formulates photoinitiator 369 and ITX, polyethylene glycol, and photocurable monomer PEGmA into a clean beaker. It was stirred with a magnetic stirrer until the photoinitiator 369 and ITX were completely dissolved. It is then added with the inhibitor according to the formula, and stirring is continued until the inhibitor is completely dissolved. When it forms a transparent and uniform solution 1, it needs to be sealed for later use. 369 is a photoinitiator with high sensitivity range and high UV absorption, which belongs to the cleavage type photoinitiator [22].

369 is often used to initiate free radical photopolymerization and is light yellow powdery crystal. Its structural formula is shown in Figure 6.

ITX is a highly efficient hydrogen abstraction photoinitiator, which is light yellow crystalline powder. Its pseudonym is isopropylthioxanthone, and its structural formula is shown in Figure 7.

369 is not only a cleavage free radical photoinitiator, but also a hydrogen-donating polymer photoinitiator, which can donate hydrogen to the hydrogen abstraction initiator ITX. Therefore, 369 is often compounded with ITX as a coinitiator, which can improve the initiation efficiency [23]. The volatilization of some components in the reaction material not only affects the performance of the reaction material but also causes pollution to the environment and harm to the human body. Therefore, the volatilization rate is also a factor that must be considered for the reaction material.

Table 2 shows the volatilization rates of the reacted materials with a monomer concentration of 75 wt% stored at 55°C in different environments for different times. It can be seen from Table 2 that after the reaction material was stored at 55°C for 72 h, the volatilization rate was only 0.72% in the highest case. Therefore, the reactive functional material has good long-term spraying stability and can meet the requirements of long-term spraying.

3.6. Properties of Water-Soluble Photocurable Reactive Materials before Curing. As mentioned above, viscosity is an important process parameter that determines whether the reaction material can be smoothly and stably ejected from the nozzle. If the viscosity is too high, the required shear force is too large, and the reaction material will not be ejected from the nozzle smoothly. If the viscosity is too low, it is easy to cause ink leakage, thus affecting the molding quality and accuracy [24]. Therefore, the reactive material should have a suitable viscosity to ensure the smooth progress of photocuring 3D printing. The suitable viscosity range in this experiment is 10~25 mPa·s. There are many factors that affect viscosity, but the most important are temperature and monomer content.

A photocurable reaction material with a monomer content of 75 wt% was prepared, and the effect of temperature on the viscosity of the reaction material was studied. At the same time, the photocurable monomer PEGmA was prepared into reaction materials with contents of 60 wt%,

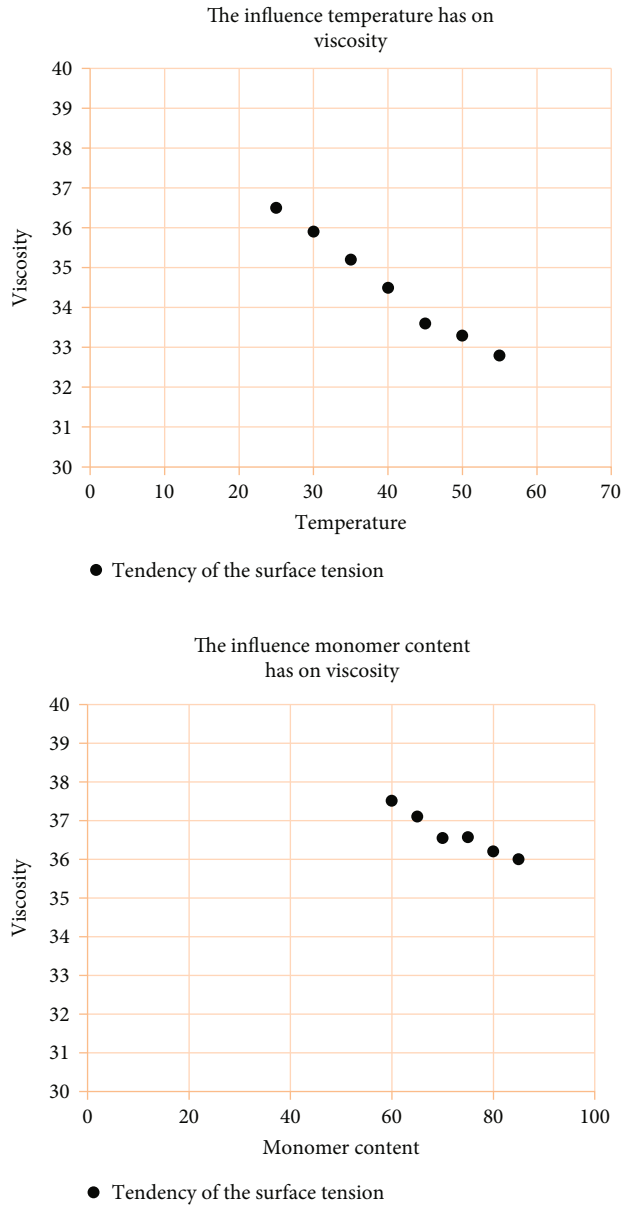

Figure 9: Effect of temperature and monomer content on the surface tension of reactive materials.

65 wt%, 70 wt%, 75 wt%, 80 wt%, and 85 wt%, respectively, and the effect of monomer content on the viscosity of the reaction material was studied. The results are shown in Figure 8.

It can be seen from Figure 8(a) that describing the effect of temperature on the reaction material, as the temperature increases, the viscosity of the reaction material gradually decreases, but the decreasing range gradually decreases. When the temperature reaches the interval of 45-60 degrees, the viscosity tends to be stable around 30. This is because the temperature increases, the intermolecular distance in the reaction material solution increases, the interaction force weakens, the resistance decreases, and the viscosity decreases. However, when the temperature is too high, the activity of the monomers in the reaction material solution increases, and a curing reaction is likely to occur. This causes the viscosity of the reaction material to rise sharply, and the solidified product of the reaction material is likely to cause clogging of the nozzle and damage the nozzle.

At the same time, Figure 8(b) shows that the viscosity of the reaction material increases gradually with the increase of the content of photocurable monomers. This is because when the content of the photocurable monomer is low, the effect of monomer molecules is weak. Each monomer molecule can be considered to exist individually, so the viscosity of the reactive material is low. However, when the monomer content is high, the intermolecular interactions of the monomers also increase significantly. At this time, the monomers no longer exist alone but exist in the solution in the form of aggregates. This in turn increases the viscosity of the solution, affecting the jetting process and part quality. Therefore, the content of monomers should be controlled to ensure the working stability of light-curing 3D printing.

Surface tension is also an important process parameter that determines whether the reaction material can be smoothly and stably ejected from the nozzle. The surface tension of the reactive material is too high, the required voltage exceeds the upper limit, and the reactive material cannot be ejected. If the surface tension is too low, the reactive material cannot form effective droplets, which affects the molding quality and accuracy. Therefore, the reaction material should have a suitable surface tension to ensure stable ejection of the reaction material. The suitable surface tension range in this experiment is 25~35 mN/m. It mainly studies the effect of temperature, monomer content, and leveling agent content on the surface tension of reactive materials [25, 26].

It prepares reactive materials with a monomer content of 75 wt% and studies the effect of temperature on the surface tension of reactive materials. It prepared the photocurable monomer PEGmA into reactive materials with contents of 60 wt%, 65 wt%, 70 wt%, 75 wt%, 80 wt%, and 85 wt%, respectively. It studies the effect of monomer content on the surface tension of reactive materials. The results are shown in Figure 9.

It can be seen from Figure 9 that with the increase of temperature, the surface tension of the reaction material gradually decreases. When the temperature exceeds 80, the surface tension drops below 36. This is because as the temperature increases, the intermolecular distance in the solution increases, the intermolecular interaction force weakens, and the surface tension decreases accordingly. But when the temperature is too high, the monomer is easy to solidify and block the nozzle. Therefore, a suitable working temperature can reduce the surface tension of the reaction material and ensure stable work. It can be seen from Figure 9 that with the increase of the content of the photocurable monomer, the surface tension of the reaction material decreases, but the decrease is smaller. This is because the pure PEGmA monomer has a low surface tension of only 32.667 mN/m. The surface tension of the solvent polyethylene glycol is as high as 57.13 mN/m. The higher the monomer content, the higher the viscosity of the reaction material. The lower the thermal stability, the easier it is to

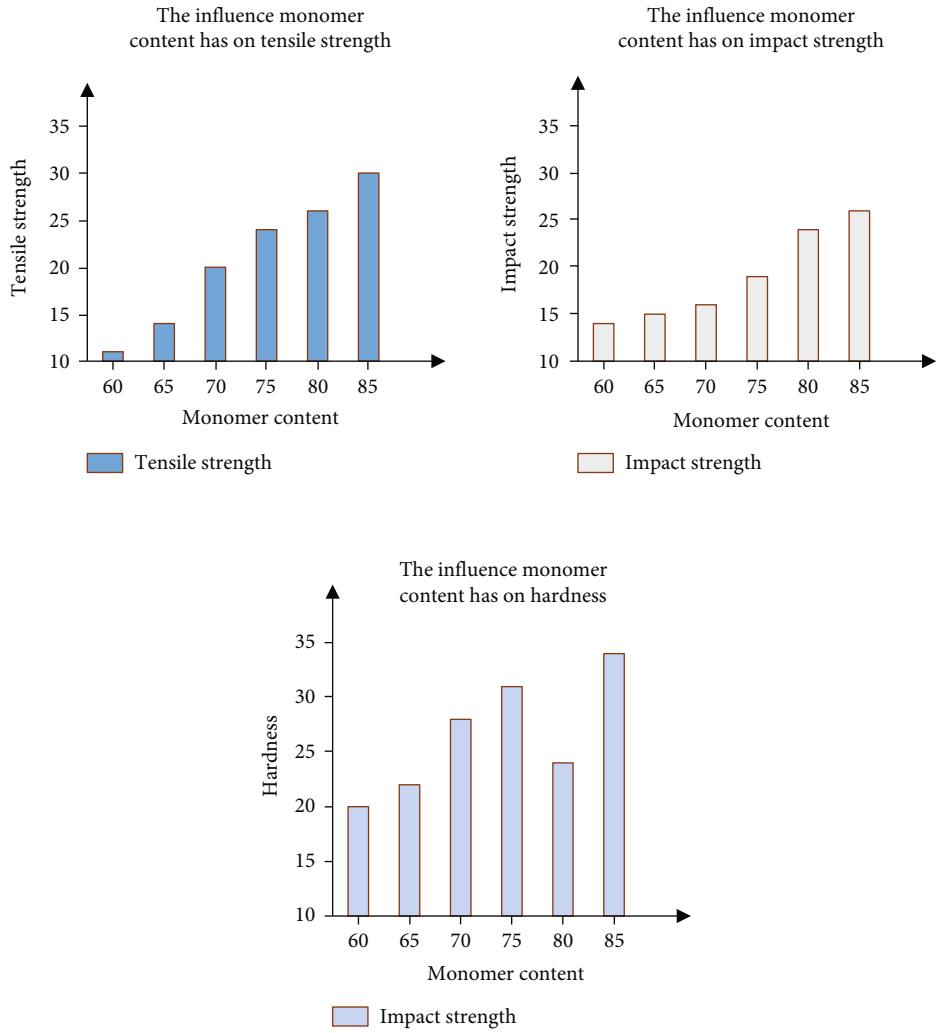

Figure 10: Effect of monomer content on surface tension, impact strength, and hardness of reactive materials.

Table 3: Effect of monomer content on hardness under different conditions.

Photocurable monomer content/wt%	60	65	70	75	80	85
Hard/HA	29	33	38	42	48	53
Soft/SA	14	18	20	29	30	39
Medium/MA	23	20	25	34	32	43

cure in advance and block the nozzle. Therefore, the higher the monomer content, the lower the solvent content, which is more conducive to the reduction of surface tension. The surface tension of the reactive material cannot be lowered by substantially increasing the monomer content [27].

3.7. Properties of Water-Soluble Photocurable Reactive Materials after Curing. There are many factors that affect the curing shrinkage of reactive materials. In this section, the effects of the content of photocurable monomers on the curing shrinkage and mechanical properties (tensile strength, impact strength, and hardness) of reactive materials are studied. It was prepared as reactive materials with monomer contents of 60 wt%, 65 wt%, 70 wt%, 75 wt%, 80 wt%, and 85 wt%, respectively. At 25°C, it studies the effect of photocurable monomer content on curing shrinkage of reactive materials.

It can be seen from Figure 10 that the higher the content of the photocurable monomer, the higher the tensile strength, impact strength, and hardness of the reaction material. This is because the photocurable monomer forms a three-dimensional space network structure after curing, which has higher mechanical properties and greater hardness. This in turn gives the reactive material suitable mechanical properties to aid in solid material shaping. Therefore, the higher the monomer content, the highest mechanical properties of the reactive material. In addition, under the influence of different environments, the reactive

Table 4: Comparison of this material with Fullcure705 and stig3.

Material types	Viscosity/ mPa·s	Tensile strength/mN/m	Volatilization rate/%	Curing shrinkage/%	Hardness/ HA	Solubility/ %
Material of this article	49.85	37.64	0.2	3.74	41	80.12
Fullcure705	71.51	33.45	0.39	0.88	26	78.6
stig3	70.49	30.88	0.51	0.66	31	69

materials are still stable. Table 3 shows the effect of monomer content on hardness under different conditions.

3.8. Performance Comparison of Water-Soluble Photocurable 3D Printing Reactive Materials and Traditionally Used Foreign Materials. In this section, the performance data of the water-soluble light-curing 3D printing materials obtained by the experiment are compared with the performance of the traditional imported commonly used materials Fullcure705 and stig3, as shown in Table 4.

It can be seen from Table 4 that the viscosity of the water-soluble photocurable reactive materials prepared in this paper is the lowest compared with the imported photocurable reactive materials Fullcure705 and stig3. It is only 49.85 mPa·s, which is beneficial to the stable ejection of the reaction material. Moreover, the surface tension is high, reaching 37.64 mN/m, which is beneficial to assist the molding of solid materials. In other properties, the solubility is as high as 80.12%, which is beneficial to the water washing and removal of the reaction material, which is also the key performance of the reaction material. And its volatilization rate is low, only 0.2%, and its mechanical properties are as high as 41HA. This is beneficial to ensure the ejection stability of the reaction material and assist the molding of the solid material. Compared with all key data, the reaction materials prepared in this paper have better comprehensive properties and are more suitable as functional materials for digital light processing 3D printing.

4. Conclusions

In this chapter, using the synthesized single-end hydroxyl PEGmA as a photocurable monomer, using its UV-curing properties and the water solubility of the cured product, and using polyethylene glycol, 369, and ITX coinitiators as raw materials, a kind of PEGmA was prepared. In addition, the curing molding mechanism and water-solubility characteristics of the material were also analyzed, the influence of each component of the material and the molding process conditions on the properties before and after curing were studied, and the optimal formulation of the water-soluble light-curing reactive material was optimized and determined. Finally, by comparing the prepared functional materials with the traditional imported materials, it is found that the materials prepared in this paper have better performance in various key indicators. In the future, the author hopes to optimize the formulation of this material through more experiments, so that it can be prepared in batches and can be used in more places.

Data Availability

Data are included within the manuscript.

Conflicts of Interest

There is no potential conflict of interest in this study.

References

[1] T. C. Huang and C. Y. Lin, "From 3D modeling to 3D printing: development of a differentiated spatial ability teaching model," *Telematics & Informatics*, vol. 34, no. 2, pp. 604–613, 2017.

[2] G. Xu, Y. Wu, T. Minshall, and Y. Zhou, "Exploring innovation ecosystems across science, technology, and business: a case of 3D printing in China," *Technological Forecasting & Social Change*, vol. 136, pp. 208–221, 2017.

[3] J. Vanderburgh, J. A. Sterling, and S. A. Guelcher, "3D printing of tissue engineered constructs for in vitro modeling of disease progression and drug screening," *Annals of Biomedical Engineering*, vol. 45, no. 1, pp. 164–179, 2017.

[4] J. Xu, L. Ding, and P. E. D. Love, "Digital reproduction of historical building ornamental components: From 3D scanning to 3D printing," *Automation in Construction*, vol. 76, pp. 85–96, 2017.

[5] D. Ho, A. Squelch, and Z. Sun, "Modelling of aortic aneurysm and aortic dissection through 3D printing," *Journal of Medical Radiation Sciences*, vol. 64, no. 1, pp. 10–17, 2017.

[6] H. W. Kim, H. Bae, and H. J. Park, "Classification of the printability of selected food for 3D printing: Development of an assessment method using hydrocolloids as reference material," *Journal of Food Engineering*, vol. 215, pp. 23–32, 2017.

[7] L. Wang, F. Zhang, Y. Liu, S. Du, and J. Leng, "Photosensitive composite inks for digital light processing four-dimensional printing of shape memory capture devices," *ACS Applied Materials and Interfaces*, vol. 13, no. 15, pp. 18110–18119, 2021.

[8] P. Upex, P. Jouffroy, and G. Riouallon, "Application of 3D printing for treating fractures of both columns of the acetabulum: benefit of pre-contouring plates on the mirrored healthy pelvis," *Orthopaedics & Traumatology: Surgery & Research*, vol. 103, no. 3, pp. 331–334, 2017.

[9] B. Bhushan and M. Caspers, "An overview of additive manufacturing (3D printing) for microfabrication," *Microsystem Technologies*, vol. 23, no. 4, pp. 1117–1124, 2017.

[10] C. Paredes, F. J. Martínez-Vázquez, A. Pajares, and P. Miranda, "Co-continuous calcium phosphate/polycaprolactone composite bone scaffolds fabricated by digital light processing and polymer melt suction," *Ceramics International*, vol. 47, no. 12, pp. 17726–17735, 2021.

[11] J. Xiao, Y. Jia, D. Liu, and H. Cheng, "Three-dimensional printing of SiCN ceramic matrix composites from preceramic

polysilazane by digital light processing," *Ceramics International*, vol. 46, no. 16, pp. 25802–25807, 2020.

[12] J. Zhang, L. Wei, X. Meng, F. Yu, and S. Liu, "Digital light processing-stereolithography three-dimensional printing of yttria-stabilized zirconia," *Ceramics International*, vol. 46, no. 7, pp. 8745–8753, 2020.

[13] J. R. Raney, B. G. Compton, J. Mueller, T. J. Ober, and J. A. Lewis, "Rotational 3D printing of damage-tolerant composites with programmable mechanics," *Proceedings of the National Academy of Sciences of the United States of America*, vol. 115, no. 6, pp. 1198–1203, 2018.

[14] R. P. Aquino, S. Barile, A. Grasso, and M. Saviano, "Envisioning smart and sustainable healthcare: 3D Printing technologies for personalized medication," *Futures*, vol. 103, pp. 35–50, 2018.

[15] I. A. Malik, M. Mirkhalaf, and F. Barthelat, "Bio-inspired "jigsaw"-like interlocking sutures: Modeling, optimization, 3D printing and testing," *Journal of the Mechanics and Physics of Solids*, vol. 102, pp. 224–238, 2017.

[16] R. J. Huang, Q. G. Jiang, H. D. Wu et al., "Fabrication of complex shaped ceramic parts with surface-oxidized Si3N4 powder via digital light processing based stereolithography method," *Ceramics International*, vol. 45, no. 4, pp. 5158–5162, 2019.

[17] D. Xue, Y. Wang, and D. Mei, "Multi-step exposure method for improving structure flatness in digital light processing-based printing," *Journal of Manufacturing Processes*, vol. 39, pp. 106–113, 2019.

[18] B. Peng, Y. Yang, K. Gu, E. J. Amis, and K. A. Cavicchi, "Digital light processing 3D printing of triple shape memory polymer for sequential shape shifting," *ACS Materials Letters*, vol. 1, no. 4, pp. 410–417, 2019.

[19] Y. Z. Yu, J. R. Lu, and L. Jing, "3D printing for functional electronics by injection and package of liquid metals into channels of mechanical structures," *Materials & Design*, vol. 122, pp. 80–89, 2017.

[20] P. Shakor, J. Sanjayan, A. Nazari, and S. Nejadi, "Modified 3D printed powder to cement-based material and mechanical properties of cement scaffold used in 3D printing," *Construction and Building Materials*, vol. 138, pp. 398–409, 2017.

[21] M. J. Ryan, D. R. Eyers, A. T. Potter, L. Purvis, and J. Gosling, "3D printing the future: scenarios for supply chains reviewed," *International Journal of Physical Distribution & Logistics Management*, vol. 47, no. 10, pp. 992–1014, 2017.

[22] T. Birtchnell, T. Bohme, and R. Gorkin, "3D printing and the third mission: the university in the materialization of intellectual capital," *Technological Forecasting & Social Change*, vol. 123, pp. 240–249, 2017.

[23] F. Naddeo, A. Naddeo, and N. Cappetti, "Novel "load adaptive algorithm based" procedure for 3D printing of lattice- based components showing parametric curved micro-beams," *Composites Part B Engineering*, vol. 115, pp. 51–59, 2017.

[24] S. Liu, Y. Li, and N. Li, "A novel free-hanging 3D printing method for continuous carbon fiber reinforced thermoplastic lattice truss core structures," *Materials & Design*, vol. 137, pp. 235–244, 2018.

[25] X. Xu, D. Shahsavari, and B. Karami, "On the forced mechanics of doubly-curved nanoshell," *International Journal of Engineering Science*, vol. 168, article 103538, 2021.

[26] X. Xu, B. Karami, and D. Shahsavari, "Time-dependent behavior of porous curved nanobeam," *International Journal of Engineering Science*, vol. 160, article 103455, 2021.

[27] L. Zeng, J. Shi, J. Luo, and H. Chen, "Silver sulfide anchored on reduced graphene oxide as a high-performance catalyst for CO_2 electroreduction," *Journal of Power Sources*, vol. 398, pp. 83–90, 2018.